UGI-97-09

The Spectral Function of the Rho Meson in Nuclear Matter *

W. Peters[1], M. Post[1], H. Lenske[1], S. Leupold[1] and U. Mosel[1,2]

[1] *Institut für Theoretische Physik, Universität Giessen, D-35392 Giessen, Germany*

[2] *Institute for Nuclear Theory, University of Washington, Box 351550, Seattle, 98195, USA*

Abstract

We calculate the modification of a rho meson in nuclear matter through its coupling to resonance-hole states. Starting from a recently proposed model, we include all four star resonances up to 1.9 GeV. In contrast to previous works, we include not only resonances that couple to the rho in a relative p-wave, but also those that couple to an s-wave state. In addition, we solve the equation for the rho spectral function self-consistently. We find that s-wave resonances affect the in medium spectral function of the rho strongly. In the transverse channel the rho meson is, especially at non zero momentum, completely washed out and can in the presence of nuclear matter no longer be viewed as a resonant excitation of the vacuum. Instead, our model shows a continuum of possible excitations with the quantum numbers of a transversely polarized rho. In the longitudinal channel, however, the rho retains its resonant character in our calculation. As a consequence of the self-consistent treatment we also find a strong enhancement of the widths of the included nucleon resonances in medium.

*Work supported by BMBF and GSI Darmstadt.

1 Introduction

There has been an ongoing discussion about the modification of the rho meson in hadronic matter for several years, but up to now the problem is not completely resolved. Due to an argument of Brown and Rho [1], based on chiral symmetry arguments and scale invariance, the mass of the rho meson should drop by about 15% at normal nuclear density. QCD sum rules arrive at a similar result, using, however, a very simple spectral function of the rho [2] (For a more detailed discussion see also [3]). Since these works link the rho mass to the scalar quark condensate, a dropping rho mass could be considered a signal for the restoration of chiral symmetry. Another argument by Pisarski [4], however, also using chiral symmetry arguments, predicts a mass that increases as chiral symmetry is restored.

All these studies use rather general concepts based on first principle arguments. A complete understanding of these effects, however, requires a reliable description of the modification of a rho meson in nuclear matter due to purely hadronic interactions and up to now there is no complete model available for this. Some works [5, 6] consider the renormalization of the $\pi\pi$ self-energy loop of the rho in medium using the delta-hole model. In [7] this approach is combined with both the works [1] and [2], and the authors claim that Brown-Rho scaling has to be introduced in order to reach consistency with the QCD sum rules. In [8], however, consistency with QCD sum rules is reached by using a chiral effective Lagrangian to calculate the rho self-energy in a $T\rho_N$ approximation without any further mass modification. In [9] a similar approximation is used to calculate a mass shift for higher three-momenta from the Compton-amplitude.

The CERES-data [10, 11, 12] caused a new discussion of this subject since theoretical models [13, 14] that used the vacuum properties of the rho clearly underestimated the dilepton yield for invariant masses in the range of about 300-600 MeV (see, however, [15]). The agreement with the data could be improved, however, by either introducing Brown-Rho scaling for the rho mass [13, 14], or by using the in-medium modification of the $\pi\pi$ loop [16].

Recently Friman and Pirner [17] calculated the contribution of resonance-hole loops to the rho self-energy in nuclear matter. In [18] this model was extended by including the $\Delta(1232)$, the modification of the $\pi\pi$ loop in medium and finite temperature effects.

In [17] only two (three in [18]) resonances were taken into account, all of

which couple to the rho in a relative p-wave. Since only p-wave resonances were included in [17], it was found that the spectral function of the rho in vacuum was restored for vanishing three-momentum since the coupling to these resonances vanishes in this limit.

We have extended the model presented in [17] by including all four-star nucleon resonances up to $m^* \sim 1.9$ GeV [19]. Several of these resonances $(N(1520), \Delta(1620), N(1650), \Delta(1700))$ can couple to the rho and a nucleon in a relative s-wave, so that also a rho meson at rest will undergo modifications because of a coupling to these channels. In this paper we explore the consequences of these new degrees of freedom and, in addition, present results of calculations in which the meson and nucleon resonance properties are treated self-consistently.

In the next section we discuss the structure of the rho-propagator in medium. In Sec. 3 we present our model for the rho self-energy, our results are shown in Sec. 4. In Sec. 5 we summarize our results.

2 The Rho-Propagator

The propagator of a free, stable spin-1 particle with mass m_o is given by:

$$\begin{aligned} D^{o\,\mu\nu}(q) &= \frac{-(g^{\mu\nu} - \frac{q^\mu\, q^\nu}{m_o^2})}{q^2 - m_o^2} \\ &= \frac{-(g^{\mu\nu} - \frac{q^\mu\, q^\nu}{q^2})}{q^2 - m_o^2} + \frac{1}{m_o^2}\,\frac{q^\mu\, q^\nu}{q^2} \quad , \end{aligned} \tag{1}$$

where in the second line of Eq. (1) we have separated the propagator into a longitudinal and a transverse part. The coupling of the rho to the pionic current gives rise to a self-energy $\Sigma^{\mu\nu}_{\pi\pi}(q^2)$. Due to current conservation, the self-energy is transverse:

$$q_\mu\, \Sigma^{\mu\nu}_{\pi\pi}(q^2) = 0 \quad . \tag{2}$$

Because of this, only the first term in Eq. (1) is modified, when a self-energy is taken into account:

$$D^{\mu\nu}(q) = \frac{-(g^{\mu\nu} - \frac{q^\mu\, q^\nu}{q^2})}{q^2 - m_o^2 - \Sigma_{\pi\pi}(q^2)} + \frac{1}{m_o^2}\,\frac{q^\mu\, q^\nu}{q^2} \tag{3}$$

with

$$\Sigma_{\pi\pi}(q^2) = -\frac{1}{3}\, g_{\mu\nu}\, \Sigma^{\mu\nu}_{\pi\pi}(q^2) \quad . \tag{4}$$

The real part of $\Sigma_{\pi\pi}$ is taken into account approximately by putting $m_o \equiv m_\rho$, where m_ρ is the physical rho-mass. Thus we take:

$$\Sigma_{\pi\pi}(q) \equiv -\mathrm{i}\; m_\rho\, \Gamma_{\pi\pi}(q^2) \quad . \tag{5}$$

$\Gamma_{\pi\pi}$ is the decay width of the rho into two pions. We use the parameterization:

$$\Gamma_{\pi\pi}(m^2) = \Gamma_o\, \frac{m_\rho}{m}\, \left(\frac{q\,(m)}{q\,(m_\rho)}\right)^3 \quad . \tag{6}$$

$q(m)$ is the momentum of the pions in the restframe of the decaying rho having mass m; m_ρ is the physical rho-mass and Γ_o the corresponding width. Eq. (6) contains precisely the energy dependence of the imaginary part of the self-energy that comes out of a one loop calculation. Since this reproduces the $\pi\pi$-scattering data up to $\sqrt{s} \sim 1$ GeV [20], we do not include an additional formfactor here, which would affect the rho width only in the region of very high invariant mass. The energy dependence of the real part of the $\pi\pi$-loop has virtually no influence on the vacuum spectral function defined as:

$$A(q^2) = -\frac{1}{\pi}\, \mathrm{Im}\left(\frac{1}{q^2 - m_\rho^2 - \Sigma_{\pi\pi}}\right) \tag{7}$$

and is therefore not included in our calculation.

In medium Lorentz-invariance is broken and the rho self-energy is characterized by two scalar functions instead of one. Using the longitudinal and transverse projectors [8]:

$$P_T^{\mu\nu} \;=\; -\begin{pmatrix} 0 & 0 \\ 0 & \delta_{ij} - \frac{q_i q_j}{\vec{q}^{\,2}} \end{pmatrix} \tag{8}$$

and

$$\begin{aligned} P_L^{\mu\nu} &= (g^{\mu\nu} - \frac{q^\mu\, q^\nu}{q^2}) - P_T^{\mu\nu} \\ &= -\begin{pmatrix} \frac{\vec{q}^{\,2}}{q^2} & \frac{\omega q_j}{q^2} \\ \frac{\omega q_i}{q^2} & \frac{\omega^2 q_i q_j}{\vec{q}^{\,2} q^2} \end{pmatrix} \end{aligned} \tag{9}$$

we can decompose the self-energy of the rho in medium:

$$\Sigma^{\mu\nu}(q) = -P_L^{\mu\nu}\,\Sigma^L(q) - P_T^{\mu\nu}\,\Sigma^T(q) \tag{10}$$

with the longitudinal and transverse parts

$$\begin{aligned} \Sigma^L(\omega,\vec{q}) &= -\;\; P_L^{\mu\nu}\Sigma_{\mu\nu}(\omega,\vec{q}) \\ \Sigma^T(\omega,\vec{q}) &= -\tfrac{1}{2}\;\; P_T^{\mu\nu}\Sigma_{\mu\nu}(\omega,\vec{q}) \quad . \end{aligned} \tag{11}$$

Then the dressed rho propagator becomes:

$$D^{\mu\nu}(\omega,\vec{q}) = -\frac{P_L^{\mu\nu}}{q^2 - m_\rho^2 - \Sigma^L(\omega,\vec{q})} - \frac{P_T^{\mu\nu}}{q^2 - m_\rho^2 - \Sigma^T(\omega,\vec{q})} + \frac{q^\mu q^\nu}{m_\rho^2 q^2} \quad . \tag{12}$$

Thus a transverse and a longitudinal spectral function can be defined:

$$A^{T(L)}(\omega,\vec{q}) = -\frac{1}{\pi}\,\mathrm{Im}\left(\frac{1}{q^2 - m_\rho^2 - \Sigma^{T(L)}(\omega,\vec{q}) - \Sigma_{\pi\pi}(q^2)}\right) \quad . \tag{13}$$

For $\vec{q} = 0$, $A^T = A^L$ is obtained.

3 The Rho Self-Energy in Matter

Similar to the pion, that becomes renormalized by delta-hole loops in the nuclear medium, there are contributions to the self-energy of the rho by resonance-hole loops. Since we are interested in a broad range of energies, there will be several resonances contributing. We include all four-star resonances up to an energy of 1.905 GeV. Only the $N(1440)$, for which the partial decay width into a rho and a nucleon is poorly known and compatible with zero [19, 21], is excluded. The resonances we include are listed in Table 1 together with their quantum numbers.

As in [17, 18] we calculate the loop contributions to the self-energy of the rho in nuclear matter in a non-relativistic approximation. The non-relativistic coupling terms are constructed by reduction of relativistic interaction Lagrangians that are compatible with parity conservation and gauge

invariance. Depending on the quantum numbers of the resonance we arrive at the following interactions:

$$\begin{aligned}
\mathcal{L}_{int} &= \tfrac{f_{RN\rho}}{m_\rho}\, \psi_R^\dagger\, \sigma_k\, \epsilon_{ijk}\, q_i\, \rho_j\, \psi \qquad \text{for} \quad \tfrac{1}{2}^+ \\
&= \tfrac{f_{RN\rho}}{m_\rho}\, \psi_R^\dagger\, S_k\, \epsilon_{ijk}\, q_i\, \rho_j\, \psi \qquad \text{for} \quad \tfrac{3}{2}^+ \\
&= \tfrac{f_{RN\rho}}{m_\rho}\, \psi_R^\dagger\, (\sigma_k\, \rho_k\, \omega - \rho_o \sigma_k\, q_k)\, \psi \quad \text{for} \quad \tfrac{1}{2}^- \\
&= \tfrac{f_{RN\rho}}{m_\rho}\, \psi_R^\dagger\, (S_k\, \rho_k\, \omega - \rho_o S_k\, q_k)\, \psi \quad \text{for} \quad \tfrac{3}{2}^- \quad .
\end{aligned} \tag{14}$$

S_k is the spin-$\frac{3}{2}$ transition operator. The isospin parts of the coupling terms are:

$$\begin{array}{ll}
\chi_R^\dagger\, \sigma_k\, \rho_k\, \chi & \text{for} \quad I = \frac{1}{2} \\
\chi_R^\dagger\, S_k\, \rho_k\, \chi & \text{for} \quad I = \frac{3}{2}
\end{array} \quad . \tag{15}$$

χ_R, χ and ρ stand for the isospin part of the wavefunction of the resonance, the nucleon and the rho, respectively.

All these couplings are current conserving, i.e. they yield zero under the replacement $\rho_\mu \to q_\mu = (\omega, \vec{q})$. This has to be the case since the rho self-energy has to fulfill the condition of current conservation, Eq. (2), in medium as well. For the $\Delta(1905)$ with $J^P = \frac{5}{2}^+$ we take:

$$\mathcal{L}_{int} = \tfrac{f_{RN\rho}}{m_\rho}\, \psi_R^\dagger\, R_{ij}\, q_i\, \rho_j^T\, \psi \quad . \tag{16}$$

In this equation R_{ij} is the spin-$\frac{5}{2}$ transition operator [17] and ρ_j^T stands for the transverse projection of the rho polarization vector:

$$\rho_j^T = \left(\delta_{jk} - \frac{q_j q_k}{\vec{q}^{\,2}}\right) \rho_k \quad . \tag{17}$$

This projection is necessary to ensure current conservation. In [17] this coupling is given without the projection onto transverse polarizations, but since only the transverse spectral function is calculated there, it is effectively taken into account.

Note that those resonances decaying into a rho in a relative p-wave have a coupling proportional to $\vec{q}$, the three momentum of the rho, while the ones coupling to an s-wave state contain $\vec{q}$ and ω, the energy of the rho. In the case $\vec{q} = 0$ only the latter will contribute. Since in [17, 18] only p-wave resonances are taken into account, in these works the vacuum propagator is recovered for $\vec{q} = 0$. If s-wave resonances are included, this is no longer the case (see sec. 4).

The coupling constants $f_{RN\rho}$ are determined by calculating the partial decay width of each resonance for a decay into a nucleon and two pions via the rho (see Fig. 1):

$$\begin{aligned} \Gamma(m_{_R}) \;&= \left(\tfrac{f_{RN\rho}}{m_\rho}\right)^2 \tfrac{1}{\pi}\, S_\Gamma \\ &\times \int_{2m_\pi}^{m_{_R}-m_{_N}} dm\; m\; \tfrac{m_N}{m_{_R}}\; |\vec{q}|^3\; A(m^2)\; F(\vec{q}^{\,2}) \end{aligned} \tag{18}$$

for p-wave decays and

$$\begin{aligned} \Gamma(m_{_R}) \;&= \left(\tfrac{f_{RN\rho}}{m_\rho}\right)^2 \tfrac{1}{\pi}\, S_\Gamma \\ &\times \int_{2m_\pi}^{m_{_R}-m_{_N}} dm\, m\; \tfrac{m_N}{m_{_R}}\; |\vec{q}|\,(2\omega^2 + m^2)\; A(m^2)\; F(\vec{q}^{\,2}) \end{aligned} \tag{19}$$

for s-wave decays.

$q(m)$ denotes the three-momentum of the rho in the center of mass frame, ω its energy and m its invariant mass. $m_{_N}(m_{_R})$ is the mass of the nucleon (the resonance). S_Γ stands for the factor arising from spin/isospin summation, its values are also given in Table 1. $A(m^2)$ is the vacuum spectral function from Eq. (7) and $F(\vec{q}^{\,2})$ is a monopole formfactor:

$$F(\vec{q}^{\,2}) = \frac{\Lambda^2}{\Lambda^2 + \vec{q}^{\,2}} \quad \text{with} \quad \Lambda = 1.5\,\text{GeV}. \tag{20}$$

The coupling constants $f_{RN\rho}$ are then adjusted to reproduce the partial decay widths [19]; together with these widths they are given in Table 1. Since the $\Delta(1232)$ does not show a measurable branching ratio into two pions,

its coupling to the rho cannot be determined by calculating a decay width. Instead, we take the value also used in [18]. The $NN\rho$ coupling constant is also taken to be the same as in [18].

For invariant masses of the resonances above their free mass, the rho-widths can become very large. This is mainly due to phase space, that becomes larger for increasing invariant mass of the resonance. To avoid unphysical values, we cut them off at 1 GeV. The precise value of this cutoff has only very little influence on our results shown in sec. 4.

Now we have all the ingredients necessary to calculate the resonance-hole loops given in Fig. 2:

p-wave resonances: Evaluating the diagrams in Fig. 2 we find for resonances with positive parity:

$$\Sigma^{ij}(\omega,\vec{q}) = \left(\delta^{ij} - \frac{q^i\,q^j}{\vec{q}^{\,2}}\right)\,\left(\frac{f_{RN\rho}}{m_\rho}\right)^2\,\vec{q}^{\,2}\,F(\vec{q})\;\;S_\Sigma\;\;\beta(\omega,\vec{q}) \tag{21}$$

and

$$\Sigma^{\mu 0} \;=\; \Sigma^{0\nu} \;=\; 0 \tag{22}$$

$\Sigma^{\mu\nu}$ as given in Eq. (21) is obviously current conserving and purely transverse. The spin-isospin factors S_Σ are also given in Table 1. The function $\beta(\omega,\vec{q})$ is given by:

$$\beta(\omega,\vec{q}) = \\ -\int_0^{p_F}\frac{d^3p}{(2\,\pi)^3}\;\left(\frac{1}{\omega - E_{_N}(\vec{p}) + E_{_R}(\vec{p}+\vec{q})} + \frac{1}{-\omega - E_{_N}(\vec{p}) + E_{_R}(\vec{p}-\vec{q})}\right) \tag{23}$$

In the limit of small nuclear density $\rho_{_N}$ or large meson momenta ($|\vec{q}| \gg p_F$), $\beta(\omega,\vec{q})$ reduces to:

$$\beta(\omega,\vec{q}) = \frac{1}{2}\,\rho_{_N}\,\frac{E_{_R}(\vec{q}) - m_{_N}}{\omega^2 - (E_{_R}(\vec{q}) - m_{_N})^2} \quad . \tag{24}$$

$E_{_N}(\vec{q})$ and $E_{_R}(\vec{q})$ are given by:

$$\begin{aligned} E_{_N}(\vec{q}) &= \sqrt{m_{_N}^2 + \vec{q}^{\,2}} \\ E_{_R}(\vec{q}) &= \sqrt{m_{_R}^2\; + \vec{q}^{\,2}} - \tfrac{\mathrm{i}}{2}\,\Gamma_{_R} \quad . \end{aligned} \tag{25}$$

$\Gamma_{_R}$ is the total width of the resonance, it is taken to be the sum of the width for pion and rho decay:

$$\Gamma_{_R} = \Gamma_{_{R\to N\pi}} + \Gamma_{_{R\to N\rho}} \quad . \tag{26}$$

$\Gamma_{_{R\to N\rho}}$ is calculated according to Eq. (18), $\Gamma_{_{R\to N\pi}}$ is taken to be

$$\Gamma_{_{R\to N\pi}} = \Gamma_o \left(\frac{q}{q_r}\right)^{2\ell+1} \quad . \tag{27}$$

q and q_r are the three momenta of a pion for a resonance of given mass and on its mass shell, respectively. ℓ is the orbital angular momentum of this pion. The values for Γ_o are given in Table 1; they are adjusted such that Γ_R from Eq. (26) is equal to the total empirical width. We find that the actual momentum dependence in Eq. (27) has only very little influence on our results (see sec. 4).

s-wave resonances: For the case of s-waves, i.e. negative parity states, one gets:

$$\Sigma^{\mu\nu}(\omega,\vec{q}) = T^{\mu\nu}\left(\frac{f_{RN\rho}}{m_\rho}\right)^2 F(\vec{q}^{\,2})\;\; S_\Sigma\;\; \beta(\omega,\vec{q}) \quad . \tag{28}$$

This expression is evaluated in the same way as for p-wave resonances. The tensor $T^{\mu\nu}$ is given by

$$T^{\mu\nu} = \begin{pmatrix} \vec{q}^{\,2} & \omega q_j \\ \omega q_i & \omega^2\delta_{ij} \end{pmatrix} \quad , \tag{29}$$

and can be expressed in terms of the projectors from Eqs. (8) and (9):

$$T^{\mu\nu} = -\omega^2 P_T^{\mu\nu} - q^2 P_L^{\mu\nu} \quad . \tag{30}$$

It follows, that the contribution of s-wave resonances to Σ^T is proportional to ω^2, while their contribution to Σ^L goes like $q^2 = \omega^2 - \vec{q}^{\,2}$. For $\vec{q} = 0$, this ensures that $\Sigma^T = \Sigma^L$, since the contribution from p-wave resonances vanishes in this case (Eq. (21)). Thus, a longitudinally polarized rho will be modified only by s-wave resonances, while a transverse rho couples to both s- and p-wave resonances.

In [18] Landau-Migdal parameters are introduced in the expressions (21) to account for additional short-range correlations. The value of these parameters for resonances beyond the $\Delta(1232)$ can, however, only be guessed. Anyway, we find that the dependence of our results on the inclusion of Landau-Migdal parameters for p-wave resonances beyond the $\Delta(1232)$ is negligible. For the $\Delta(1232)$ we take:

$$\Sigma_\Delta(\omega,\vec{q}) \;=\; \frac{\Sigma_\Delta^o}{1-g'\frac{\Sigma_\Delta^o}{\vec{q}^2}} \tag{31}$$

with $g'=0.5$.

The spectral function in Eq. (13) contains the rho-width of the resonances, which in turn contains the spectral function via Eq. (18) and (19). This implies a change of the rho decay-width of a resonance in medium. We solve this problem self-consistently by iterating Eq. (13), starting with the vacuum spectral function. The first step of this iteration is equivalent to the calculations in [17].

The resonance widths in medium are given in terms of the two spectral functions A^T and A^L by:

$$\begin{aligned}\Gamma(m_{_R}) \;&=\Big(\tfrac{f_{RN\rho}}{m_\rho}\Big)^2\,\tfrac{1}{2\pi}\,S_\Gamma\;\int q\;dq\;d\cos\theta \\ &\times\;\; \tfrac{m_N}{E_N}\;|\vec{q}|^3\;A^T(\omega,\vec{q})\;F(\vec{q}^{\,2})(1-n_f(\vec{q}))\end{aligned} \tag{32}$$

for p-wave resonances and

$$\begin{aligned}\Gamma(m_{_R}) \;&=\Big(\tfrac{f_{RN\rho}}{m_\rho}\Big)^2\,\tfrac{1}{2\pi}\,S_\Gamma\;\int q\;dq\;d\cos\theta \\ &\times\;\; \tfrac{m_N}{E_N}\;|\vec{q}|\,(2\omega^2A^T(\omega,\vec{q})+m^2A^L(\omega,\vec{q}))\;\;F(\vec{q}^{\,2})(1-n_f(\vec{q}))\end{aligned} \tag{33}$$

for s-wave resonances. $\cos\theta$ is the emission angle of the rho in the cm-frame of the decaying resonance and q is its three-momentum. In the vacuum, i.e. for $A^L=A^T$, this reduces to the expressions (18) and (19).

4 Results and Discussions

Within the framework described in the previous sections we have calculated the spectral functions A^T and A^L of the rho meson in nuclear matter.

In order to make the interpretation of the following figures easier, we show in Fig. 3 the free dispersion relations for the rho, the $\Delta(1232)$, the $N(1520)$ and the $N(1720)$, since these are the resonances that can be identified most easily in the following plots. For the resonances m stands for the invariant mass that a meson of given momentum must have in a collision with a nucleon at rest in order to excite the respective resonance on its mass shell.

In Fig. 4 we show A^T as a function of three-momentum and invariant mass of the rho when only p-wave resonances are included, as the result of a non self-consistent calculation. This spectral function can be directly compared to that obtained by Friman and Pirner [17]. Even though these authors include only two resonances, their result is qualitatively similar to the one shown in Fig. 4. At $\vec{q} = 0$ the spectral function is equal to the one in vacuum, while for higher momenta the rho-peak vanishes and a new structure appears at lower invariant masses, which stems from the $\Delta(1232)$ and the $N(1720)$. It must be kept in mind, that the value of the $\Delta N\rho$ coupling constant is rather uncertain, so that only qualitative conclusions can be made about its contribution.

Including also the s-wave resonances leads to a drastic change of A^T, especially at small $\vec{q}$ (upper part of Fig. 5). The rho-peak is strongly depleted also for small momenta and a pronounced, sharp new ridge due to the $N(1520)$ appears at lower invariant masses and momenta. The dominance of this branch is due to the relatively large observed partial decay width of the $N(1520)$ of about 25 MeV into a rho and a nucleon [19]. Since the resonance mass lies far below the energetic threshold for this decay calculated from the peak mass of the rho, this decay can proceed only through the tails of the rho-mass distribution leading to a relatively large coupling constant.

In the lower part of Fig. 5 we show the corresponding longitudinal spectral function A^L. Again, the $N(1520)$ leads to a pronounced structure at small $\vec{q}$. In contrast to A^T in the upper part of this Figure, the $N(1520)$-branch dies out for increasing $\vec{q}$. The rho-branch is reappearing at higher invariant mass, but its peak is reduced by a factor of two relative to the vacuum case. The vanishing of the $N(1520)$-branch is due to the fact, that the contribution of s-wave resonances to Σ^L is proportional to $q^2 \equiv m^2$ (see Eq. 30), which decreases along the $N(1520)$-branch as shown in Fig. 3. This m^2-dependence, together with the fact, that the rho-branch and the resonance branches become the more separated, the higher the momentum is (see Fig. 3), is also the reason why the rho-branch reappears in the longitudinal channel. This

is in contrast to the contribution of s- and p-wave resonances to Σ^T, that goes with ω^2 and $\vec{q}^{\,2}$, respectively. Both these factors increase along a line of constant m in Fig. 5, and lead therefore to the very broad distribution of strength for large $\vec{q}$ in the case of A^T.

Using the coupling given in Eq. (14) for $\frac{1}{2}^+$ resonances, we find that an (NN^{-1}) loop yields only a negligible contribution to the rho self-energy.

In all the calculations shown, we integrate over the Fermi-sphere of the nucleons in medium instead of using the approximation (24). We find, however, that this has only very little effect on the final result. Using Eq. (24) would lead to slightly sharper resonance peaks in Fig. 5, but would not change any of the dominant features. This shows that our calculation so far amounts essentially to taking into account the linear term in an expansion of the self-energy into powers of the nuclear density $\rho_{_N}$, which is equivalent to considering reactions of the rho with only a single nucleon. This is a reasonable assumption as long as the three-momentum is high enough, so that the rho can actually resolve a single nucleon. For vanishing three momentum, however, this is not the case, so that terms of higher order in the density, i.e. reactions with more than one nucleon, will become important. These are contained in a self-consistent solution that includes terms to an arbitrary order in the density, or, phrased differently, reactions of the rho with an arbitrary number of nucleons.

The result for such a self-consistent calculation is shown in Figs. 6 and 7 for normal nuclear density. For higher three-momenta there are only small changes in both A^T and A^L, while for $\vec{q} \to 0$ there is a strong influence of the terms of higher order in the density. The main effect is that the structures visible in Fig. 5 at small $\vec{q}$ are washed out.

In the lower parts of Figs. 6 and 7 we show cuts through the upper parts of these figures for different three momenta together with the vacuum spectral function. Note that in Fig. 6, in particular for momenta $|\vec{q}| > 0.2$ GeV, the transverse spectral function does not exhibit a resonance-like structure, so that a description of the in-medium rho in terms of mass and width is no longer appropriate for transverse polarization. In contrast to that, the longitudinal spectral function still shows a resonant behavior, especially for $|\vec{q}| > 0.4$.

Thus we find, that at finite $\vec{q}$ a transverse rho undergoes a stronger modification than a longitudinal one. The reason is that only s-wave resonances contribute to the longitudinal channel, and their effect decreases with in-

creasing $\vec{q}$. The transverse channel on the other side, is also modified by p-wave resonances, whose contributions to the rho self-energy increase (see above). This difference between the polarizations agrees qualitatively with the findings of QCD sum rules at finite $\vec{q}$ [24], as well as the analysis in [9].

While these different polarizations of the rho could be exploited in experiments using polarized particles, e.g. real, transverse photons, in the incoming beam, for the description of heavy-ion collisions only the statistically averaged spectral function $A = \frac{1}{3}(2A^T + A^L)$ is relevant. In Fig. 8 we show A in the same way as A^L and A^T in Figs. 6 and 7. At $\vec{q} = 0$, we have $A = A^L = A^T$; for higher momentum a maximum coming from the longitudinal rho is still visible, but it sits upon a strong transverse background.

The self-consistent calculation has another surprising consequence, namely that, except for the $\Delta(1232)$, the rho decay-widths of the resonances increase dramatically. This is easy to understand, since there is more strength in the region of small invariant masses of the rho, where the phase space for the decay becomes larger. The values of these partial widths in vacuum for on-shell resonances are given in Table 2, together with the values resulting from a non-selfconsistent calculation, as well as a self-consistent calculation at two different nuclear densities. The difference between the free value and the result of the non-selfconsistent calculation is due to Pauli-blocking in the medium. The widths for $\rho_N = 2\rho_o$ are smaller than for normal nuclear density due to the increasing importance of Pauli-blocking. In addition, one sees from Fig. 3, that the branches of $\Delta(1232)$ and $N(1520)$ dive down into the region with $m^2 < 0$, so that the overall amount of transverse strength in the region relevant for the resonance decay ($m^2 > 4m_\pi^2$), decreases.

The results in Table 2 are for resonances with $\vec{q} = 0$; we find only a moderate dependence of these widths on the three-momentum. The $\Delta(1232)$ is practically left unchanged, its rho-width stays below 1 MeV.

As already discussed in [22] the significant broadening of the nucleon resonances with large rho-decay widths also contributes to the observed disappearance of the nucleon resonances beyond the Delta in the total photoabsorption cross sections on nuclei [25]. While Fermi-motion alone already leads to a significant broadening of the absorption cross section on the individual, in particular the higher-lying, resonances, it is not sufficient to explain the disappearance of the $N(1520)$. This resonance which has a large electromagnetic strength is just the one that is broadened the most in our calculation. Also other effects, such as the onset of the 2π channel, contribute most proba-

bly to the disappearance of the $N(1520)$ in the photoabsorption cross section; a quantitative evaluation of this mechanism, however, so far does not exist.

Fig. 9 shows A calculated self-consistently for a density $\rho_{_N} = 2\rho_o$. One sees that the ridge coming from the $\Delta(1232)$ becomes more prominent, since its contribution to the self-energy increases (cf. Eqs. (23) and (24)), but it is not broadened like the other resonances (see above). At the same time, higher invariant masses are even more depleted. For higher $\vec{q}$ the rho branch is still visible, but it is much weaker than for $\rho_{_N} = \rho_o$ (Fig. 8). The peak at $\vec{q} = 0$ in the region of the $N(1520)$, which acquires a large width in medium, is due to the fact that the rho-strength of the N(1520) depends very strongly on the mass of this resonance because of its 'subthreshold' character. Since this mass is lowered at the higher density, the rho-channel opens up and the strength increases significantly.

We now explore the sensitivity of our results to additional effects on the rho in medium, that are not yet included. First, the modification of the $\pi\pi$-loop has to be considered. In [5, 6] the authors show, that this leads mainly to a broadening of the rho. In the upper part of Fig. 10 we therefore show A as the result of a self-consistent calculation employing twice the vacuum value for the decay width of the rho. The effect is, that around $m = m_\rho$ the strength is smeared out somewhat more, the rho-peak is less pronounced. The qualitative behavior of A remains unaltered.

Second, there still could be a possible change of the mass-parameter in the propagator of the rho. This might be due to a Brown-Rho type scaling, or due to t-channel interactions of the rho with the nucleon as e.g. considered in [23]. In the lower part of Fig. 10 we therefore show results of a calculation employing a rho mass (see Eq. (13)) that is lowered by 100 MeV. The rho peak at high $\vec{q}$ is shifted by 100 MeV, while at small momentum a stronger shift to lower invariant masses is visible.

The negative parity resonances, that we assume to couple to a rho in an s-wave state, lead to a strong effect in our calculation. They can in principle also couple to a rho in a relative d-wave, which would again vanish for $\vec{q} = 0$. The main effect on the rho spectral function, however, comes from the $N(1520)$ and in the analysis [21] the coupling of this resonance to the rho is clearly determined to be s-wave. Besides, for the decay of a resonance into a nucleon and a massive meson like the rho, the higher waves will be the more suppressed, the lighter the resonance is.

5 Summary and Conclusions

We have calculated the transverse and longitudinal spectral functions of the rho meson in nuclear matter in a model that includes the interaction of the rho with the medium via resonance-hole loops. In extension to earlier works, we include all resonances up to 1.9 GeV. We find that the so far neglected s-wave resonances, especially the $N(1520)$, have a very strong influence on the spectral functions, especially for small three-momentum of the rho. We have performed a self-consistent calculation by iterating the equation for the spectral functions. This amounts to including terms of arbitrary order in the nuclear density. We find that the self-consistent treatment of the rho has a strong effect for small three-momentum of the rho, but leaves both longitudinal and transverse spectral function more or less unchanged for $|\vec{q}| > 0.5$ GeV. In the transverse channel the rho-peak vanishes completely and a large amount of strength is shifted to smaller invariant masses. Besides a ridge coming from the $\Delta(1232)$, no structure can be seen anymore; we find a continuum of transverse excitations with the quantum numbers of the rho. For the longitudinal spectral function we find a different behavior: Being equal to the transverse one for $\vec{q} = 0$, it shows a clear peak stemming from the rho meson for $|\vec{q}| > 0.5$ GeV, which is reduced by a factor of two relative to the vacuum.

As a side result of our self-consistent calculation, we find that simultaneously the widths of the resonances with rho-nucleon decay branches are drastically enhanced in medium due to the fact that the rho spectral function shows much strength at small invariant masses; only the $\Delta(1232)$ is left unchanged. Since these are just those resonances that also have large electromagnetic couplings (vector meson dominance!) this behavior will contribute to the observed disappearance of the higher-lying nucleon resonances beyond the $\Delta(1232)$ in the total photoabsorption cross section on nuclei

We conclude, that the resonant nature of a transverse rho meson vanishes completely in medium, leading to a strong enhancement at small invariant masses. The higher the three momentum of the rho, the broader is the distribution of the transverse strength, while in the longitudinal case the rho branch is still visible for $|\vec{q}| > 0.5$. Thus we find, that a simple scaling law of the rho-mass and perhaps the width, that does not distinguish between longitudinal and transverse polarization, cannot account for the effect of hadronic interactions on the properties of the rho in medium.

6 Acknowledgments

One of the authors (U.M.) thanks the Institute for Nuclear Theory at the University of Washington for its hospitality and the U.S. Department of Energy for partial support during completion of this work.

References

[1] G.E. Brown and M. Rho, Phys. Rev. Lett. **66** (1991) 2720.

[2] T. Hatsuda and S.H. Lee, Phys. Rev. **C46** (1992) R34.

[3] S. Leupold, W. Peters and U. Mosel, in preparation.

[4] R. Pisarski, Phys. Rev. **D52** (1995) R3773.

[5] M. Herrmann, B. Friman and W. Nörenberg, Nucl. Phys. **A545** (1992) 267c ; Nucl. Phys. **A560** (1993) 411.

[6] G. Chanfray and P. Schuck, Nucl. Phys. **A545** (1992) 271c ; Nucl. Phys. **A555** (1993) 329.

[7] M. Asakawa, C.M. Ko, P. Lévai and X.J. Qiu, Phys. Rev. **C46** (1992) R1159; M. Asakawa and C.M. Ko, Phys. Rev. **C48** (1993) R526.

[8] F. Klingl and W. Weise, hep-ph/9704398.

[9] V.L. Eletsky and B.L. Ioffe, Phys. Rev. Lett. **78** (1997) 1010.

[10] G. Agakichiev et al., CERES collaboration, Phys. Rev. Lett. **75** (1995) 1272.

[11] A. Drees for the CERES collaboration, in Proc. of the International Workshop XXV on QCD Phase Transitions, Hirschegg 1995, eds. H.Feldmeier et al., (GSI Darmstadt 1997), p. 178.

[12] N. Masera for the HELIOS-3 collaboration, Nucl. Phys. **A590** (1995) 93c.

[13] W. Cassing, W. Ehehalt and C. M. Ko, Phys. Lett. **B363** (1995) 35.

[14] G.Q. Li, C.M. Ko and G. E. Brown, Phys. Rev. Lett. **75** (1995) 4007; Nucl. Phys. **A606** (1996) 568.

[15] V. Koch and C. Song, Phys. Rev. **C54** (1996) 1903.

[16] R. Rapp, G. Chanfray and J. Wambach, Phys. Rev. Lett. **76** (1996) 368.

[17] B. Friman and H.J. Pirner, Nucl. Phys. **A617** (1997) 496.

[18] R.Rapp, G. Chanfray and J. Wambach, Nucl. Phys. **A617** (1997) 472.

[19] Particle Data Group, Phys. Rev. **D54** (1996) 1.

[20] F. Klingl, N. Kaiser and W. Weise, Z. Phys. **A356** (1996) 193.

[21] D.M. Manley and E.M. Saleski, Phys. Rev. **D45** (1992) 4002.

[22] M. Effenberger, A. Hombach, S. Teis and U. Mosel Nucl. Phys. **A613** (1997) 353.

[23] B. Friman and M. Soyeur, Nucl. Phys. **A600** (1996) 477.

[24] S.H. Lee, nucl-th/9705048.

[25] N. Bianchi et al., Phys. Lett. **B325** (1994) 333.

	$I(J^P)$	Γ_π $[MeV]$	Γ_ρ $[MeV]$	l_ρ	$f_{RN\rho}$	S_Γ	S_Σ
N(940)	$\frac{1}{2}(\frac{1}{2}^+)$	0	0	1	7.7	6	4
N(1520)	$\frac{1}{2}(\frac{3}{2}^-)$	95	25	0	7.0	1	8/3
N(1650)	$\frac{1}{2}(\frac{1}{2}^-)$	135	15	0	0.9	3	4
N(1680)	$\frac{1}{2}(\frac{5}{2}^+)$	118	12	1	6.3	3/5	6/5
N(1720)	$\frac{1}{2}(\frac{3}{2}^+)$	50	100	1	7.8	2	8/3
Δ(1232)	$\frac{3}{2}(\frac{3}{2}^+)$	120	0	1	15.3	2/3	16/9
Δ(1620)	$\frac{3}{2}(\frac{1}{2}^-)$	130	20	0	2.5	1	8/3
Δ(1700)	$\frac{3}{2}(\frac{3}{2}^-)$	180	120	0	5.0	1/3	16/9
Δ(1905)	$\frac{3}{2}(\frac{5}{2}^+)$	140	210	1	12.2	1/5	4/5

Table 1: List of the resonances included in this calculation together with the parameters used. The third and fourth columns contain the values we use for the pionic width of the resonances (see. Eq. 27)) and explanation thereafter) and for the rho-width. Columns five and six show the angular momentum of the rho and the coupling constants from Eq. (14). The last two columns contain the spin/isospin factors occurring in Eqs. (18,19), (21) and (28).

	$\Gamma_\rho[MeV]$			
	Vacuum	Pauli-bl.	$\rho = \rho_o$	$\rho = 2\rho_o$
N(1520)	25	7	240	200
N(1650)	15	5	35	20
N(1680)	12	8	90	60
N(1720)	100	85	560	330
Δ(1620)	20	7	70	40
Δ(1700)	120	45	160	90
Δ(1905)	210	205	300	130

Table 2: List of the free and in-medium rho-widths of the resonances on their mass shell. The second column shows the free value we start from, the third column is the free width corrected for Pauli-blocking. The fourth and fifth column show the widths resulting from a self-consistent calculation of the rho spectral function for two different densities.

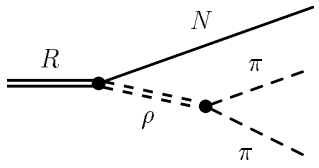

Figure 1: Decay of a nucleon resonance into two pions via a rho meson.

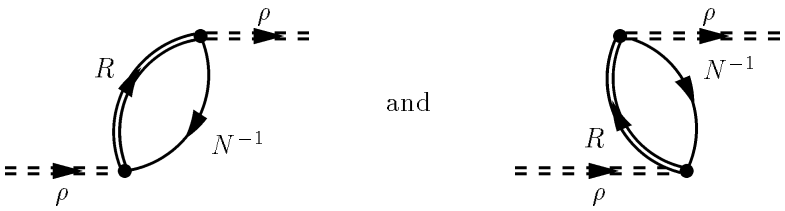

Figure 2: Resonance-hole self-energy diagrams for the rho meson. The double dashed line stands for a physical rho meson that contains the $\pi\pi$-width.

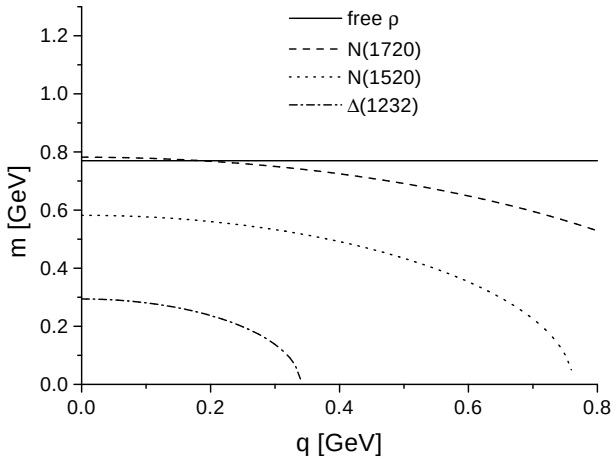

Figure 3: Free dispersion relations for the rho and the most prominent resonances. For the resonance branches m is the invariant mass a meson of given three-momentum q must have in order to excite the respective resonance on its mass shell.

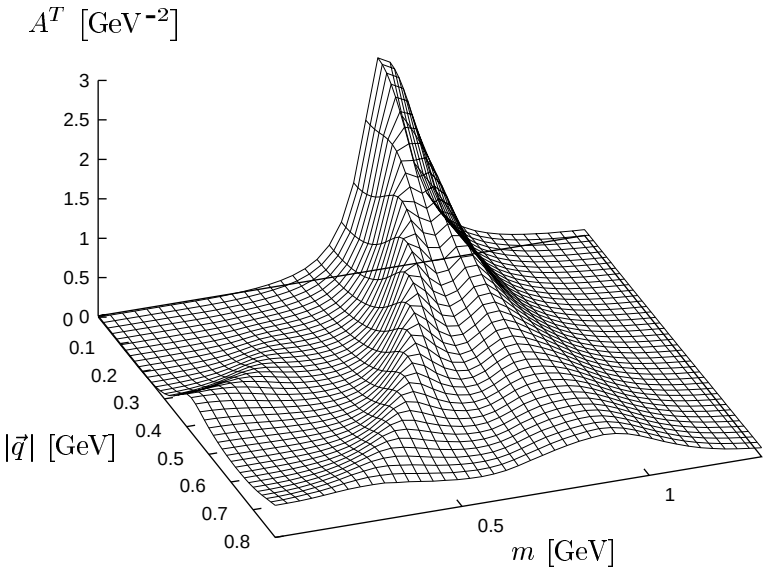

Figure 4: Non-selfconsistent transverse spectral function of the rho meson in nuclear matter as defined in the text for $\rho_{_N} = \rho_o$ as a function of invariant mass m and three-momentum q. Only p-wave resonances are included.

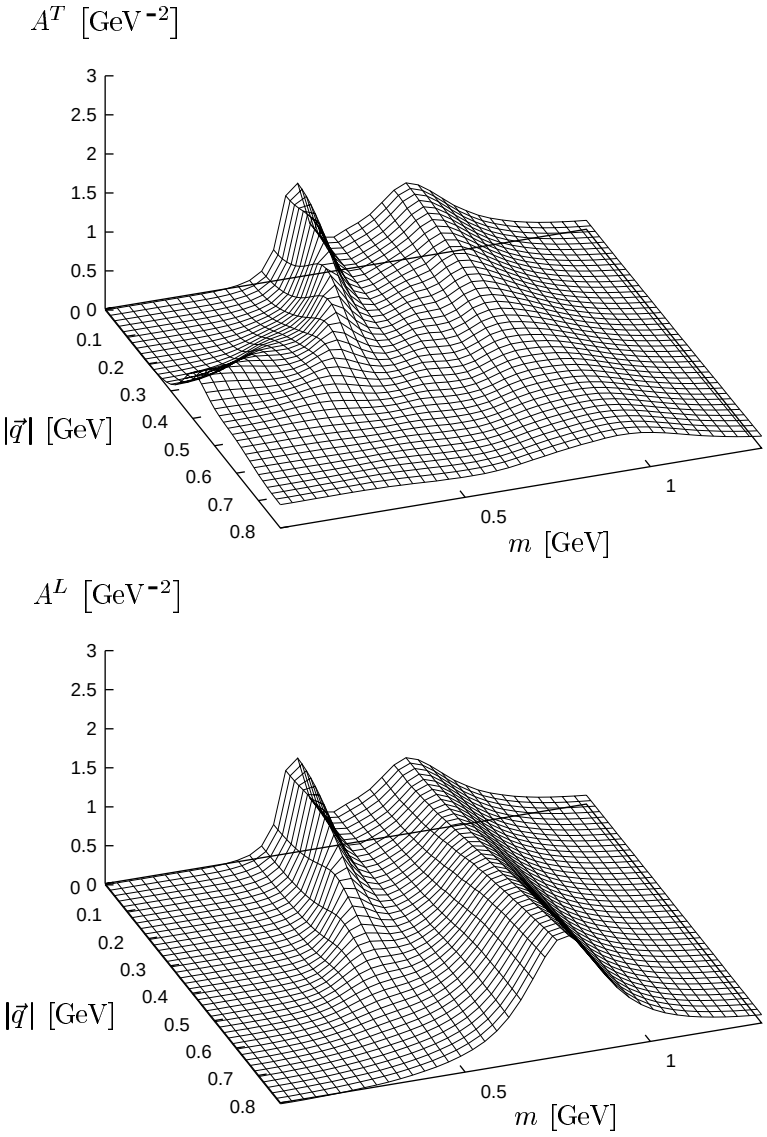

Figure 5: Non-selfconsistent spectral functions of the rho meson for $\rho_{_N} = \rho_o$. Upper part: transverse spectral function. Lower part: longitudinal spectral function.

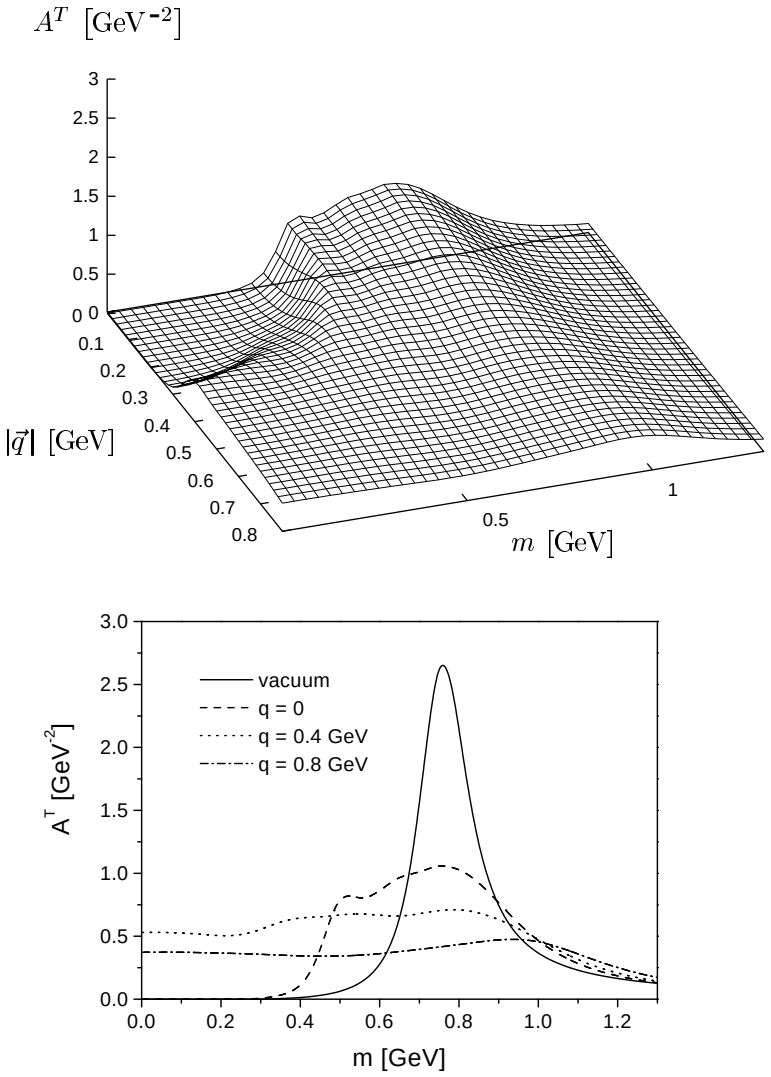

Figure 6: Self-consistent transverse spectral function of the rho meson for $\rho_N = \rho_o$. Lower part: Cuts through the upper part for different three-momenta together with the vacuum spectral function.

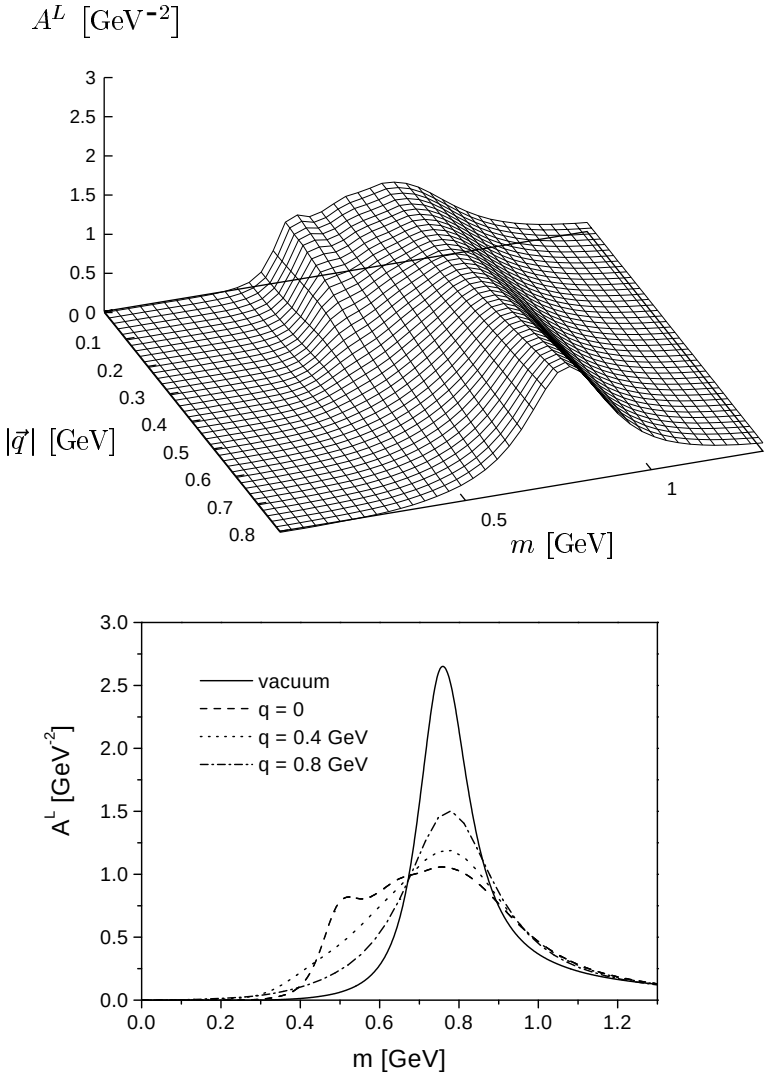

Figure 7: Same as Fig. 6, but for the longitudinal spectral function.

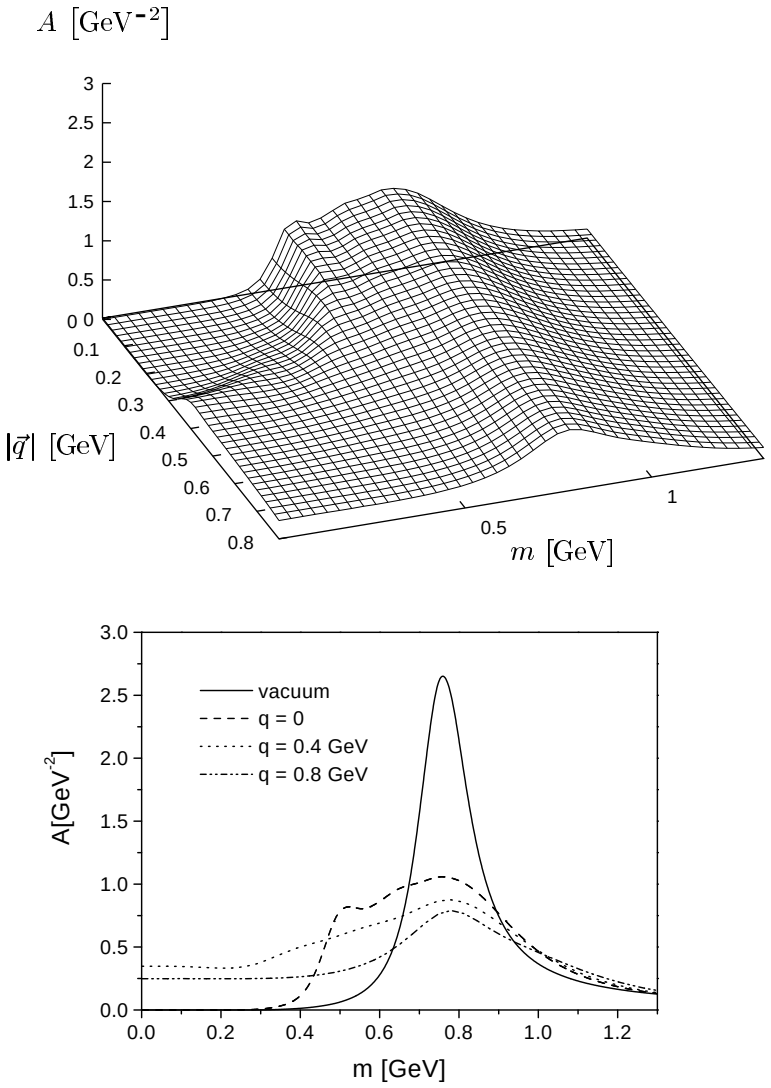

Figure 8: Same as Fig. 6, but for the averaged spectral function.

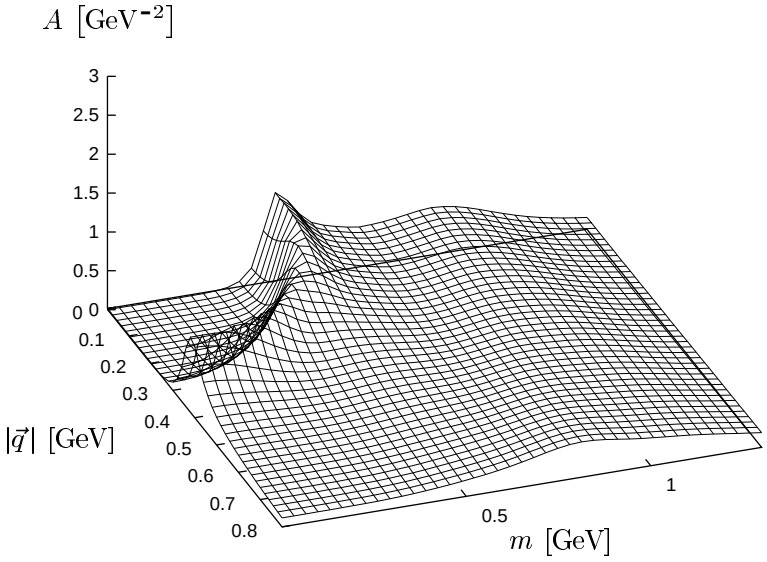

Figure 9: Self-consistent averaged spectral function of the rho meson for $\rho_{_N} = 2\rho_o$.

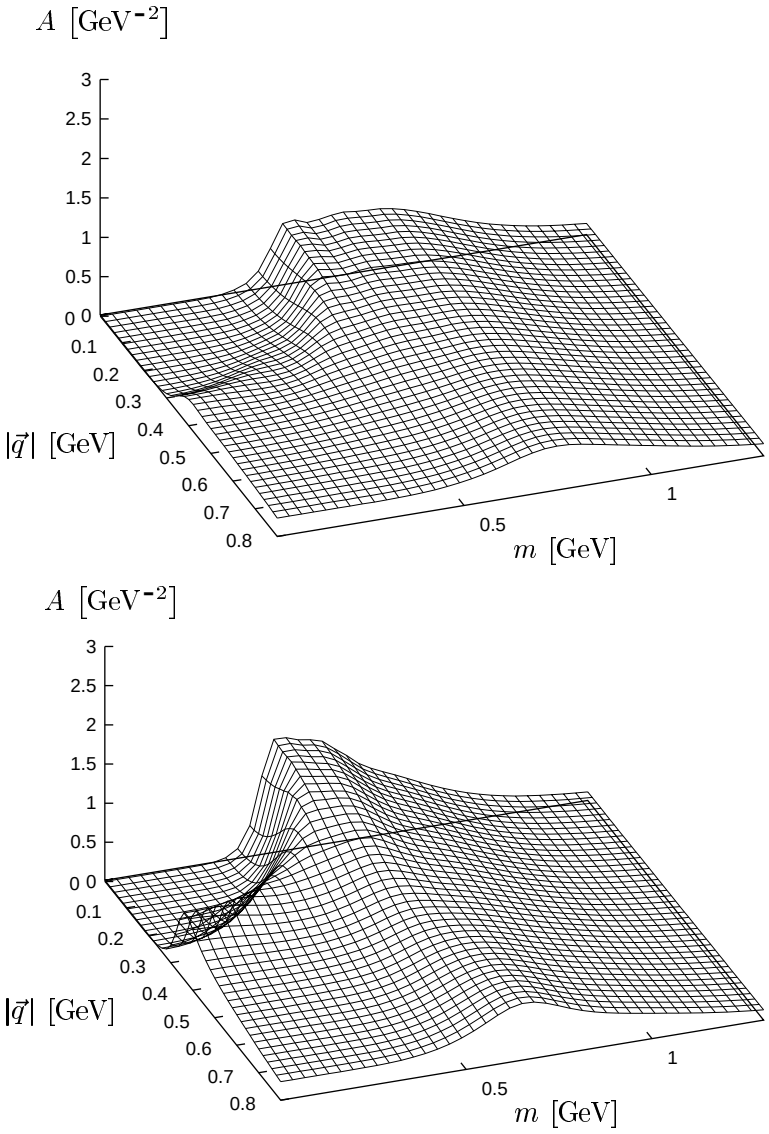

Figure 10: Self-consistent averaged spectral function of the rho meson for $\rho_{_N} = \rho_o$. Upper part: using a vacuum rho-width of 300 MeV. Lower part: using a rho mass reduced by 100 MeV.